

Figure 1. Increased sensitization and prevalence of food allergy among patients with WAS mutations. (A) Schematic of WAS with causative mutations identified among cohort (n = 25) with WAS mutations. Bolded variants indicate a diagnosis of Wiskott-Aldrich syndrome (WAS); unbolded indicate X-linked thrombocytopenia (XLT); italicized indicate mutations associated with presence of food allergy in childhood. **(B)** Total serum IgE levels and food allergen specific IgE levels among cohort; limit of detection for food specific IgE was 0.1 IU/ml. Light grey indicates the normal range; colored boxes indicate the median and interquartile range for the four foods reported in NHANES (Ref 23). White circles indicate individuals with clinically diagnosed food allergy. **(C)** Among patients with serum samples obtained prior to transplantation (n = 22), percent of WAS (n = 12) or XLT (n = 10) patients with positive serum IgE (sIgE) to foods, with a minimum cutoff of 0.35 IU/mL compared to the general population as reported in NHANES analysis (left panel). Prevalence of food allergy during childhood among all studied WAS (n = 15) and XLT (n = 10) patients compared to those reported in the general population (NHANES) and among patients with moderate to severe atopic dermatitis (AD, right panel) (Refs 24 and 25). **(D)** Concordance of sIgE measurement to skin prick testing (SPT) among individuals who underwent both SPT and sIgE testing to foods (n = 14) (left panel). Results of SPT and sIgE testing to foods among patients with clinical food allergy (n = 6) (right panel). U/D – undefined; N/D – none detected; WH1 – WASP Homology domain 1; GBD – GTP-ase binding domain; PPP – Polyproline domain; VCA – verprolin homology, cofilin homology and acidic region domain; TN – walnut and cashew.

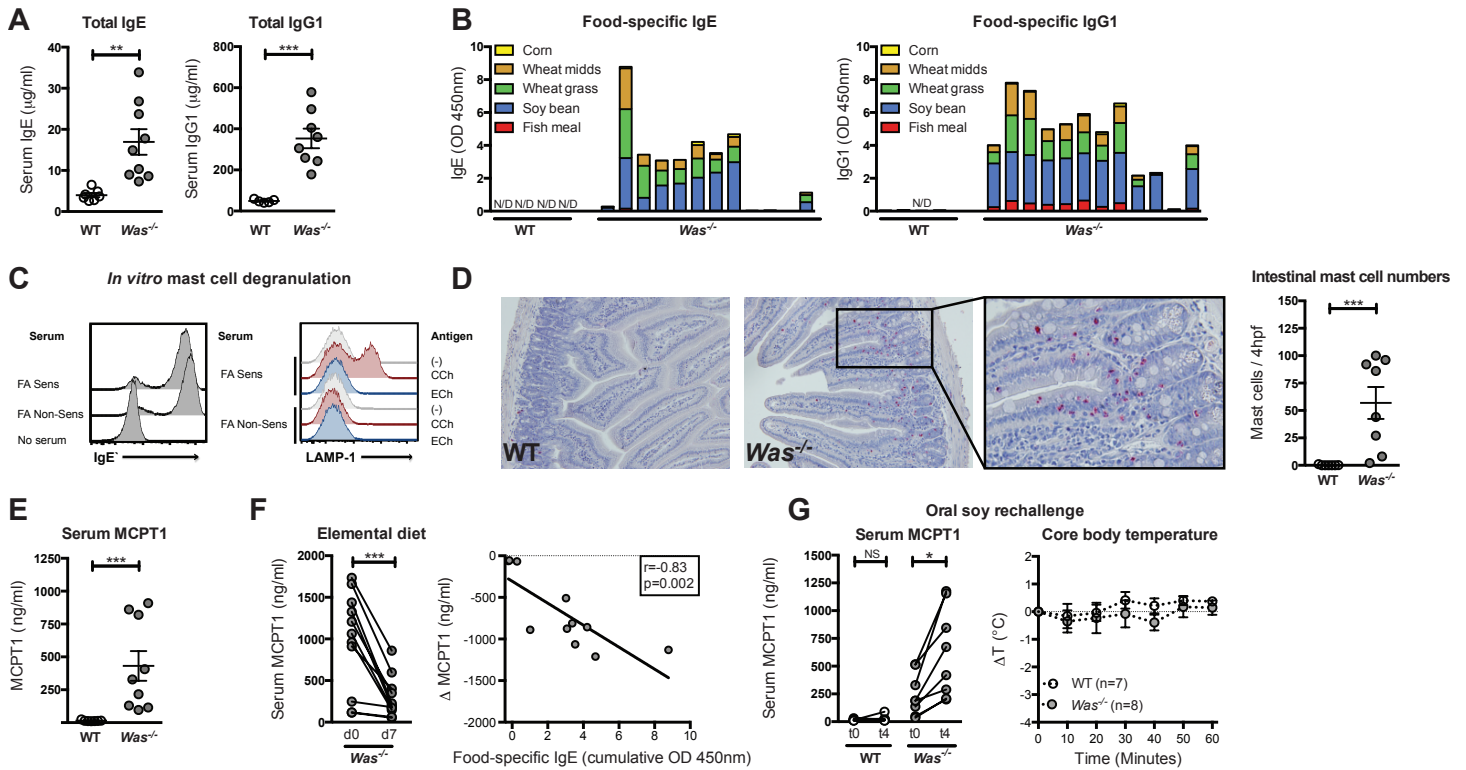
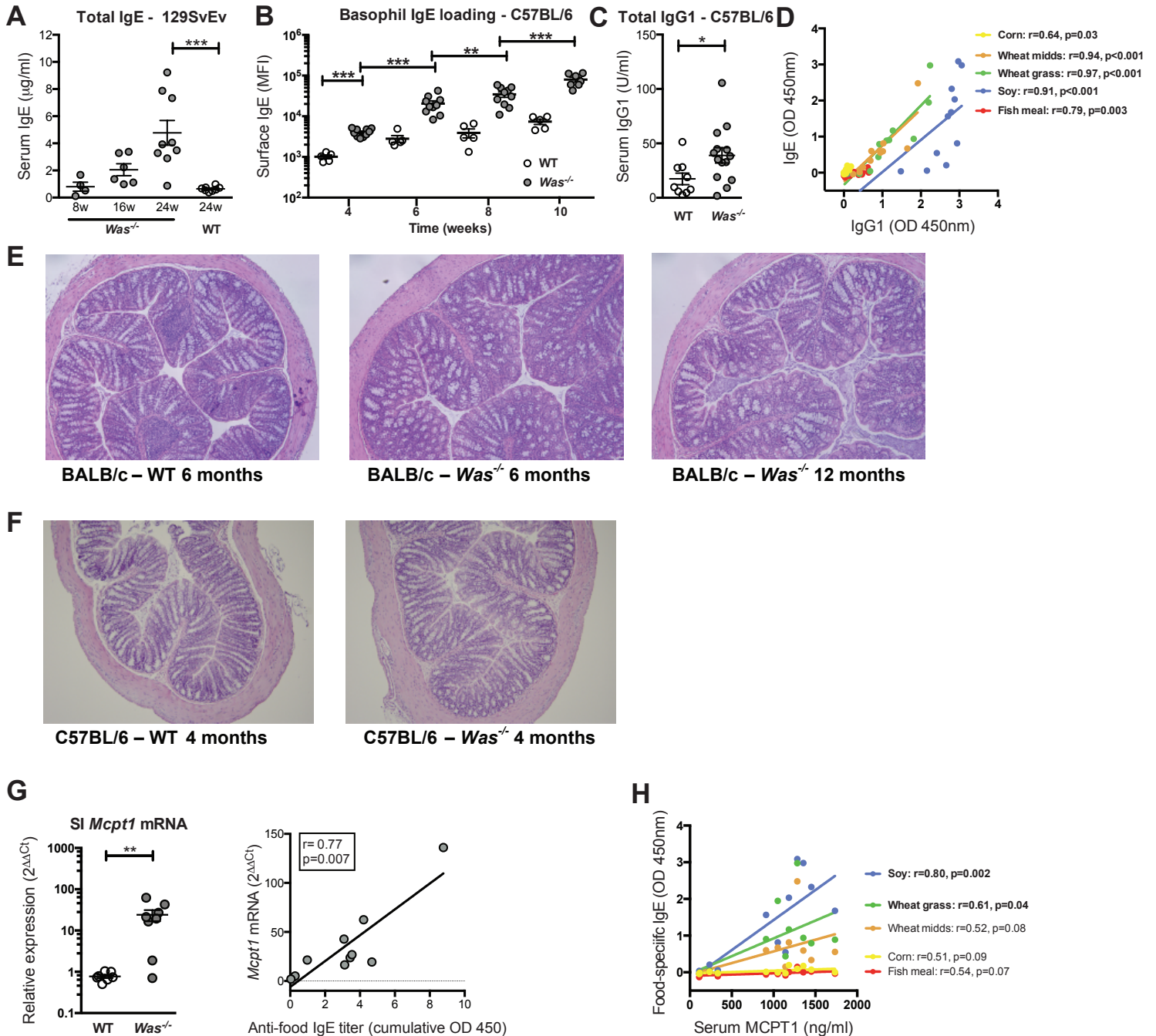


Figure 2. Spontaneous sensitization to food antigens and food allergy in *Was*^{-/-} mice. (A) Comparative analysis of total serum IgE and IgG1 levels in 3-month old WT BALB/c (open circles) and *Was*^{-/-} mice (gray circles) of mixed genders. (B) IgE and IgG1 reactivity against the five main (%w/w) chow components as determined by ELISA in 1:30 (IgE) or 1:1000 (IgG1) diluted serum samples. (C) Loading of WT bone-marrow-derived mast cells with serum of food allergic (FA Sens) or non-food allergic (FA Non-Sens) *Was*^{-/-} mice compared to no-serum control (left panel). Appearance of surface LAMP-1 as a marker of mast cell degranulation after stimulation with antigen extracts from conventional chow (CCh), elemental chow (ECh) or PBS (-). (D) Intestinal mast cell expansion as determined by chloroacetate esterase staining of jejunal cross-sections (20X) and quantification in WT and *Was*^{-/-} mice. (E) Serum levels of mast cell protease 1 (MCPT1) determined by ELISA. (F) Effect of 7-day treatment with elemental diet on serum MCPT1 in *Was*^{-/-} mice. Spearman's rank correlation between cumulative anti-food IgE titers of mice and response to allergen elimination defined as Δ MCPT1. (G) Effect of oral rechallenge with 12.5 mg soy protein extract on body temperature and serum MCPT1 after 4h. Symbols represent individual mice and error bars depict SEM. N/D: not detectable; ** $p < 0.01$; *** $p < 0.001$; NS: not significant as determined by t-test.



Supplemental Figure 1. Age-dependency of IgE levels in *Was*^{-/-} mice and absence of colonic inflammation in C57BL/6 and BALB/c *Was*^{-/-} animals. (A) Serum IgE levels in 129SvEv *Was*^{-/-} animals between 8 and 24 weeks. (A) Bi-weekly assessment of surface IgE loading on blood basophils (CD45^{Mid}CD49b⁺) from WT (open circles) and *Was*^{-/-} (gray circles) on the C57BL/6 background. (C) Total levels of serum IgG1 in C57BL/6 *Was*^{-/-} mice. (D) Pearson correlation coefficients between anti-food IgE and IgG1 titers for the five main chow components in Balb/c *Was*^{-/-} mice. (E) H&E staining of colonic cross-sections from 6-12 month old WT and BALB/c *Was*^{-/-} mice and (F) 4-month old *Was*^{-/-} mice on the C57BL/6 background. (G) Relative gene expression of *Mcpt1* in small intestinal (SI) tissue samples and correlation of *Mcpt1* mRNA expression with anti-food IgE titer. (H) Pearson correlation coefficients (r) between food-specific IgE titers and baseline serum MCPT1. Symbols represent individual mice and error bars depict SEM. * $p<0.05$; ** $p<0.01$; *** $p<0.001$; NS: not significant as determined by t-test or paired t-test for intraindividual analyses.

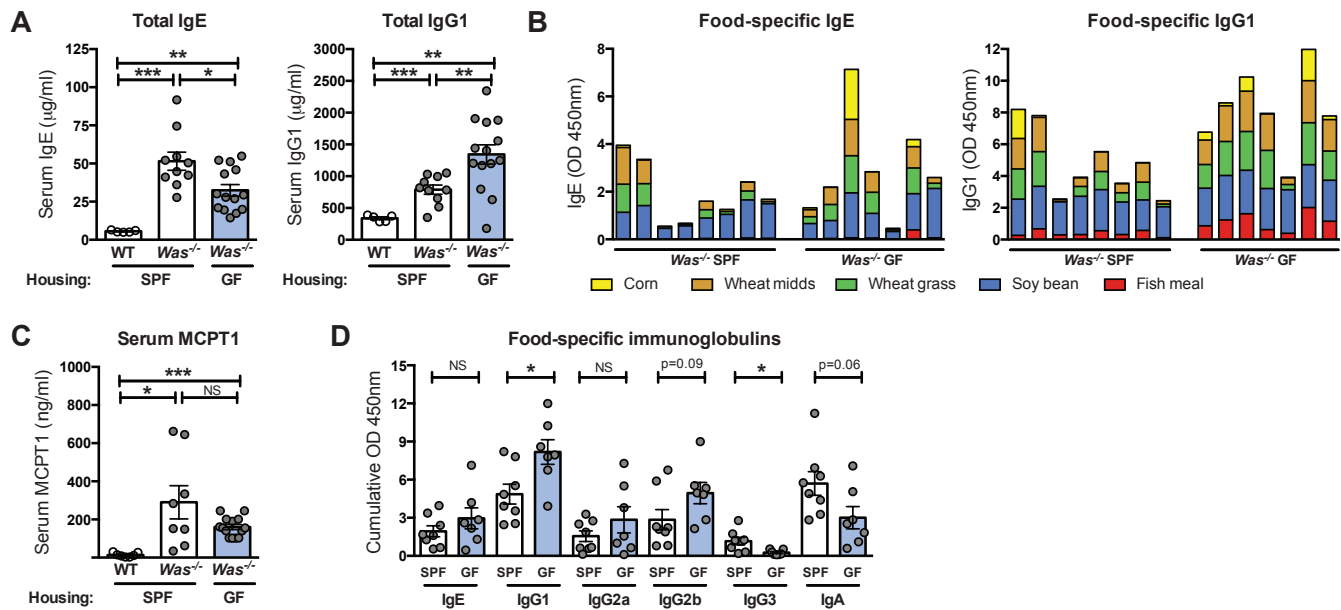
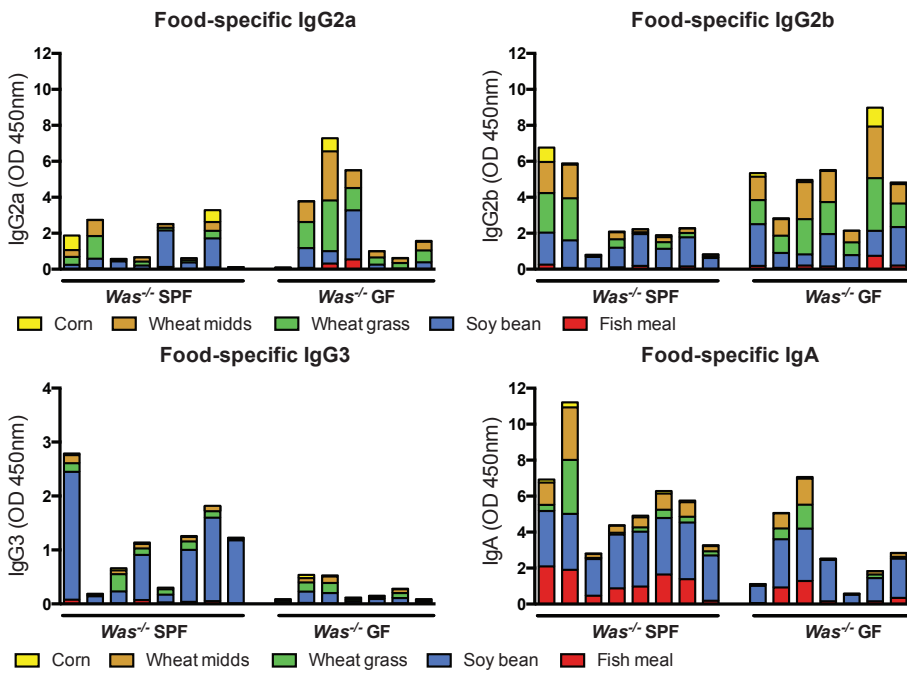
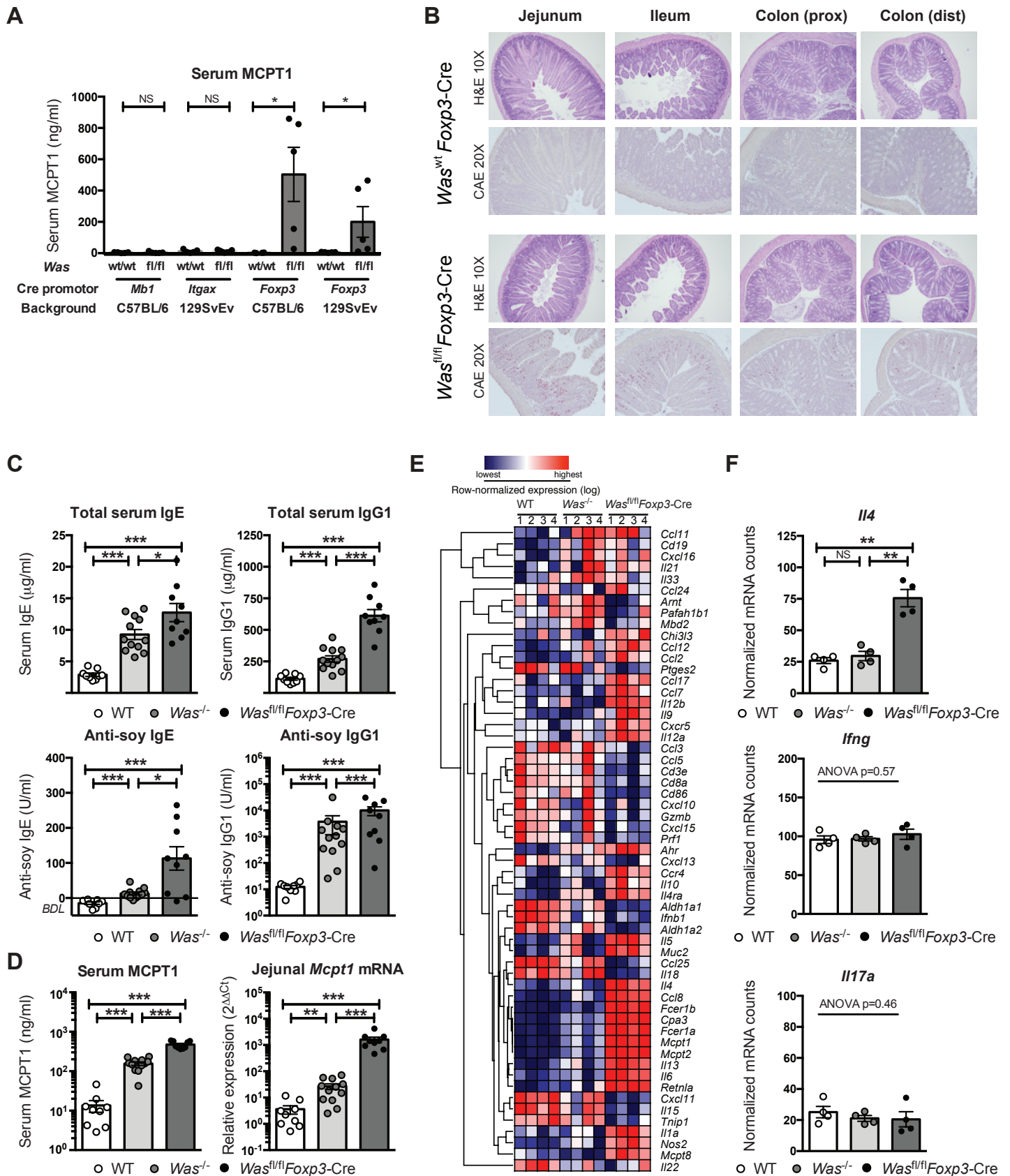


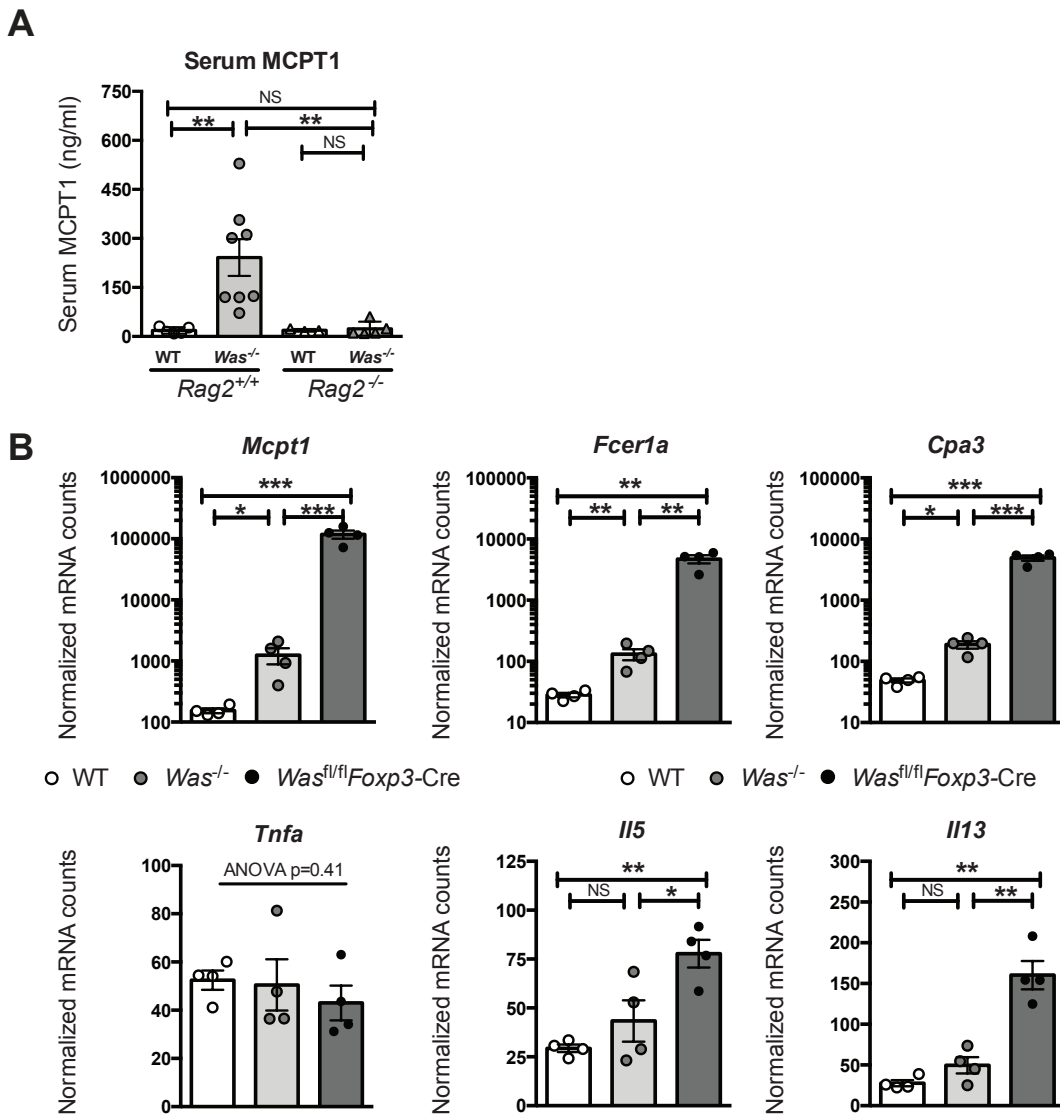
Figure 3. Commensals are dispensable for spontaneous sensitization to food in *Was*^{-/-} mice but shape the isotype composition of the humoral anti-food response. (A) Comparison of total IgE and total IgG1 serum levels in 4-6-month old WT (open circles) or *Was*^{-/-} (gray circles) on the 129SvEv background that were housed under either specific-pathogen-free (SPF) or germ-free (GF) conditions. (B) Food-specific IgE and IgG1 for the five main chow constituents in IgE (serum dilution 1:100) or IgG1 (1:5000) from SPF and GF *Was*^{-/-} mice. (C) Comparison of serum MCPT1 levels. (D) Comparison of cumulative anti-food titers of IgE, IgG1, IgG2a (1:1000), IgG2b (1:1000), IgG3 (1:200), and IgA (1:5000) in SPF and GF *Was*^{-/-} animals. Symbols represent individual mice and error bars depict SEM. *p<0.05; ** p<0.01; ***p<0.001; NS: not significant as determined by t-test. Results are shown from sera obtained from mice from ≥3 independent cohorts.



Supplemental Figure 2. Detailed analysis of food-specific titers for the five main chow constituents. Contribution of individual component-specific immunoglobulins to the cumulative anti-food isotype titers of IgG2a, IgG2b, IgG3, and IgA in SPF and GF-housed *Was*^{-/-} mice.



(*Was^{fl/fl}Foxp3-Cre*) of ≥ 2 months of age, $n \geq 5$ per group. **(B)** Representative H&E and chloroacetate staining of intestinal cross-sections in *Was^{fl/fl}Foxp3-Cre* or *Was^{wt}Foxp3-Cre* littermates on C57BL/6 background. **(C)** Comparison of total and soy-specific IgE and IgG1 at 2 months in co-housed WT (open circles, $n=9$), *Was^{-/-}* (gray circles, $n=12$), and *Was^{fl/fl}Foxp3-Cre* (black circles, $n=9$) mice of mixed genders on the C57Bl6 background. **(D)** Comparison of serum protein and jejunal mRNA expression levels of mucosal mast cell marker MCPT1. **(E)** Hierarchical cluster analysis of differentially expressed genes in a panel of 86 inflammatory targets. Row-normalized, log-transformed mRNA counts are shown from 4 animals per group. **(F)** Jejunal mRNA counts for inflammatory cytokines. Symbols represent individual mice and error bars depict SEM. * $p < 0.05$; ** $p < 0.01$; *** $p < 0.001$; NS: not significant as determined by t-test (panel A) or one-way ANOVA with Tukey's multiple comparisons test (panels C, D, F). *BDL* below detection limit.



Supplemental Figure 3. Intestinal mast cell expansion in $Was^{-/-}$ mice requires adaptive immunity and $Was^{fl/fl}Foxp3-Cre$ mice develop Th2-type intestinal inflammation. (A) Comparison of serum MCPT1 in WT (open circles, $n=5$), $Was^{-/-}$ (gray circles, $n=8$), $Rag2^{-/-}$ (open triangles, $n=3$) and $Was^{-/-}Rag2^{-/-}$ (gray triangles, $n=5$) mice ≥ 2 months old on the 129SvEv background. (B) Normalized absolute mRNA counts obtained from digital mRNA profiling of jejunal tissue for indicated genes. Symbols represent individual mice and error bars depict SEM. * $p<0.05$; ** $p<0.01$; * $p<0.001$; NS: not significant as determined by t-test (panel A) or one-way ANOVA with Tukey's multiple comparisons test (panel B).**

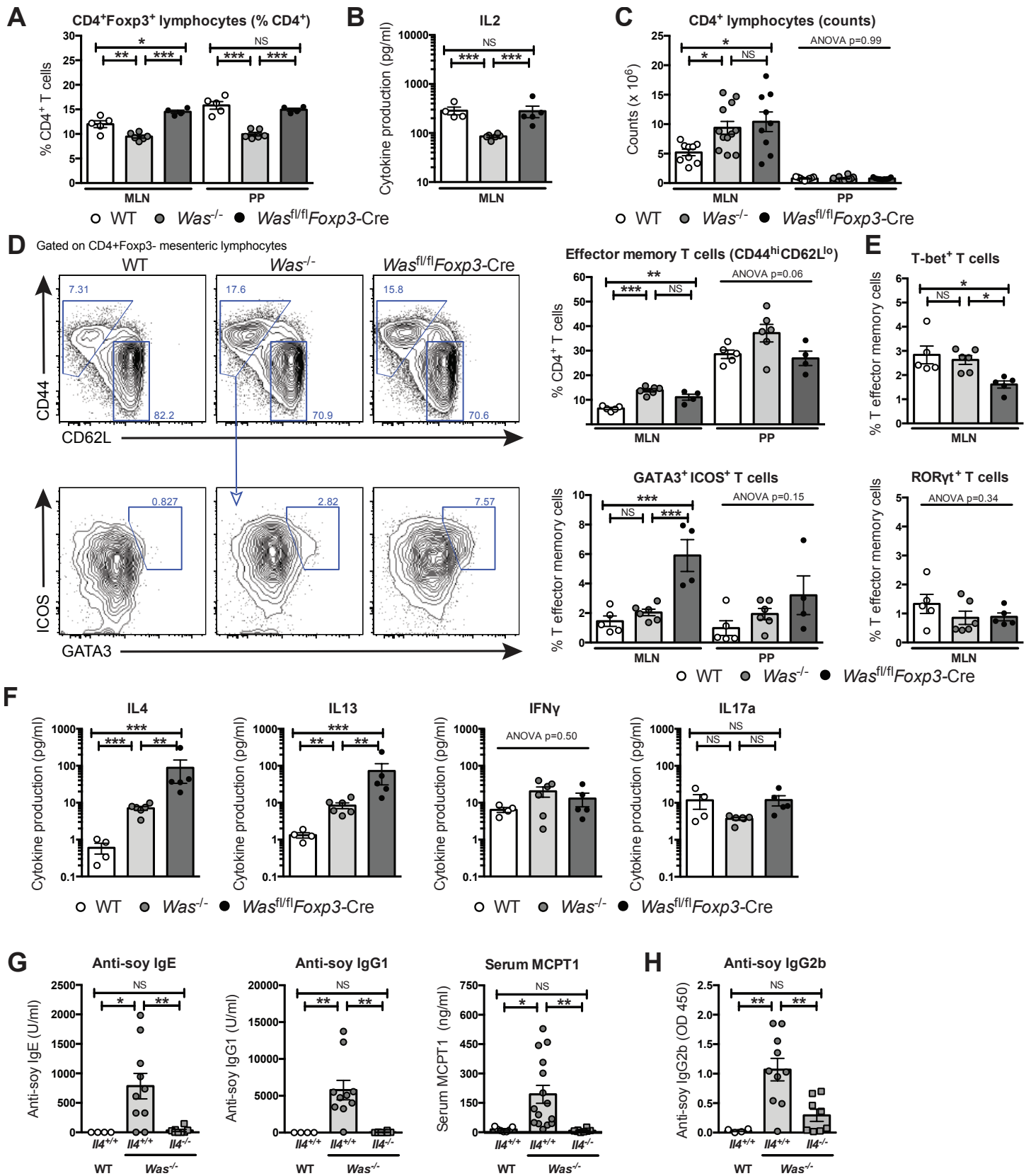
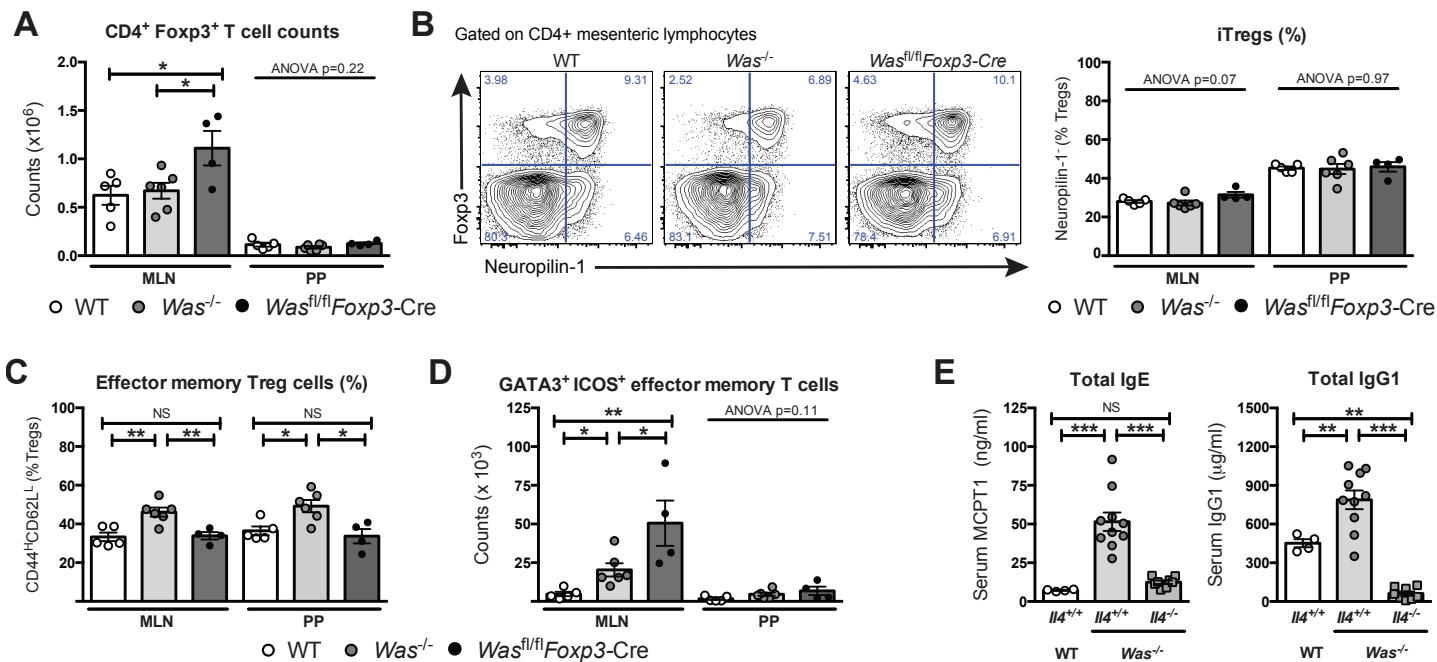


Figure 5. WASP-deficient Foxp3⁺ Tregs fail to suppress Th2 type lymphoproliferation *in vivo*. (A) Quantification by flow cytometry of Foxp3⁺ Tregs amongst CD4⁺ T cells obtained from mesenteric lymph nodes (MLNs) or Peyer's patches (PP) of WT (open circles), *Was*^{-/-} (gray circles) and *Was*^{fl/fl}*Foxp3-Cre* (black circles) mice. (B) Production of IL2 by CD4⁺ mesenteric T lymphocytes stimulated with anti-CD3/CD28 *ex vivo*. Each dot represents the average cytokine production from triplicate cell suspensions from a single mouse. (C) Total CD4⁺ T cell numbers obtained from MLN and PP. (D)

Gating strategy of GATA3⁺ICOS⁺ Th2-type effector cells within the parent gate of effector memory T cells from MLNs of representative samples, with quantification and statistical testing in the right panels. **(E)** Fraction of T-bet⁺ and RORγt⁺ effector memory T cells. **(F)** Production of IL-4, IL-13, IFN-γ and IL-17a by CD4⁺ mesenteric T lymphocytes stimulated with anti-CD3/CD28 *ex vivo*. Each dot represents the average cytokine production from triplicate cell suspensions from a single mouse. **(G)** Serum levels of anti-soy specific IgE and IgG1, and MCPT1 in *Was*^{-/-} mice on the 129SvEv background with either *Il4*^{+/+} (gray circles) or *Il4*^{-/-} alleles (gray squares). **(H)** Anti-soy IgG2b titer as determined by ELISA in 1:1000 serum dilution. Symbols represent individual mice and error bars depict SEM. *p<0.05; ** p<0.01; ***p<0.001; NS: not significant as determined by t-test or one-way ANOVA with Tukey's multiple comparisons test. In B and F, data were log-transformed prior to statistical testing. Representative results of ≥2 independent experiments.



Supplemental Figure 4. WASP-deficient Foxp3⁺ Tregs fail to suppress Th2 type lymphoproliferation *in vivo*. (A)

Quantification of Foxp3⁺ Tregs counts in MLNs and PPs of WT, Was^{-/-}, and Was^{fl/fl}Foxp3-Cre animals. (B) Gating strategy and summary statistic of the fraction of iTregs, defined as Foxp3⁺ Neuropilin-1⁻, within the total population of Tregs obtained from MLNs. (C) Summary statistic of the subpopulation of CD44^{Hi}CD62L^{Lo} effector memory Tregs within the total population of CD4⁺Foxp3⁺ lymphocytes. (D) Absolute numbers of Th2-type, GATA3⁺ICOS⁺ effector memory cells in MLNs and PPs. (E) Serum levels of total IgE and IgG1 in Was^{-/-} mice on the 129SvEv background with either Il4^{+/+} or Il4^{-/-} alleles. Symbols represent individual mice and error bars depict SEM. *p<0.05; ** p<0.01; ***p<0.001; NS: not significant as determined by t-test or one-way ANOVA with Tukey's multiple comparisons test. Representative results of ≥2 independent experiments.

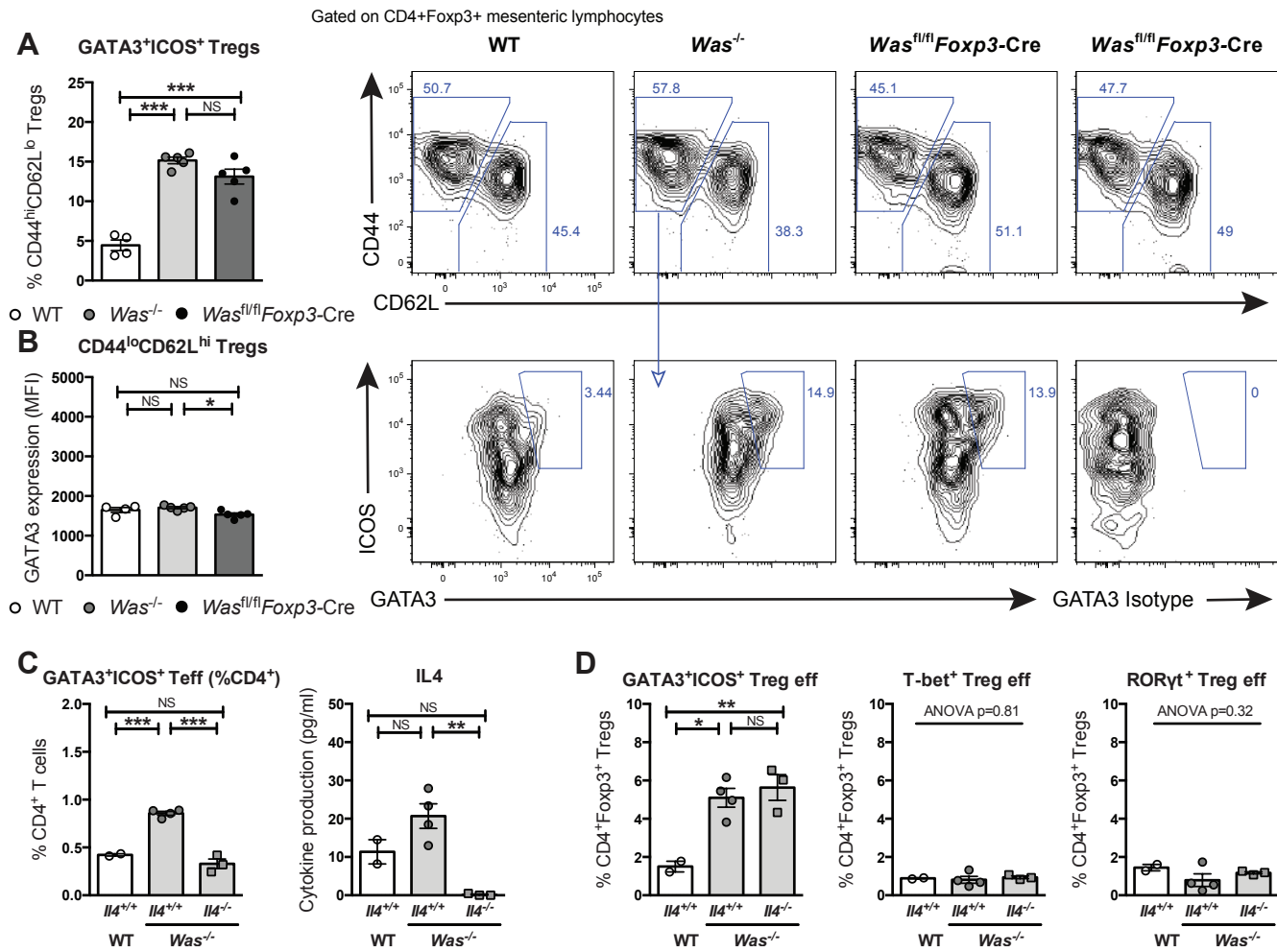
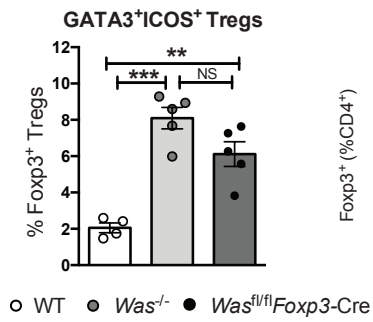
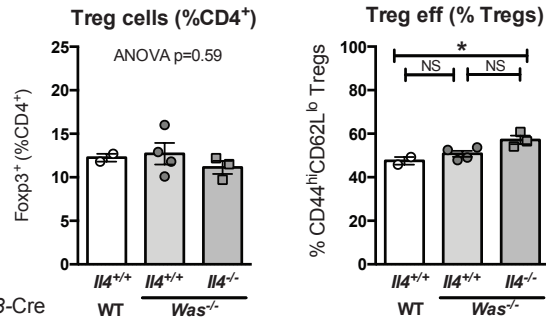


Figure 6. WASP-deficient effector Tregs assume a Th2-like phenotype. (A) Fraction of CD44^{hi}CD62L^{lo}CD4⁺Foxp3⁺ Tregs that co-express GATA3 and ICOS in WT (open circles), *Was*^{-/-} (gray circles) and *Was*^{fl/fl}Foxp3-Cre (black circles) mice, with gating strategy in representative samples depicted on the right. (B) Intracellular GATA3 levels in CD44^{lo}CD62L^{hi}CD4⁺Foxp3⁺ Tregs determined by flow cytometry. (C) GATA3⁺ICOS⁺ effector T cells in WT or *Was*^{-/-} mice with either *I14*^{+/+} or *I14*^{-/-} alleles and IL-4 production by CD4⁺ mesenteric lymphocytes stimulated with anti-CD3/CD28 *ex vivo*. Each dot represents the average cytokine production from triplicate cell suspensions from a single mouse. (D) Percentage of Foxp3⁺ Tregs co-expressing GATA3 and ICOS, T-bet, or RORγt in in WT or *Was*^{-/-} mice with either *I14*^{+/+} (gray circles) or *I14*^{-/-} alleles (gray squares). Symbols represent individual mice and error bars depict SEM. *p<0.05; **p<0.01; ***p<0.001; NS: not significant as determined by one-way ANOVA with Tukey's multiple comparisons test.

A**B**

Supplemental Figure 5. WASP-deficient effector Tregs assume a Th2-like phenotype. (A) Fraction of total CD4⁺Foxp3⁺ Tregs that co-express GATA3 and ICOS in WT, *Was*^{-/-} and *Was*^{fl/fl}Foxp3-Cre mice. (B) Fraction of Foxp3⁺ Tregs amongst CD4⁺ mesenteric lymphocytes and effector memory Tregs amongst total Foxp3⁺ Tregs in WT or *Was*^{-/-} mice with either *Il4*^{+/+} or *Il4*^{-/-} alleles on the 129sv background. Dots represent cells from individual mice and error bars depict SEM. *p<0.05; ** p<0.01; ***p<0.001; NS: not significant as determined by one-way ANOVA with Tukey's multiple comparisons test.